Title: SARS-CoV-2 20I/501Y.V1 variant in the hamster model

Author list: Maxime Cochin*[1], Léa Luciani*[1], Franck Touret[1], Jean-Sélim Driouich[1], Paul-Rémi Petit[1], Grégory Moureau[1], Cécile Baronti[1], Laurence Thirion[1], Piet Maes[2], Robbert Boudewijns[3], Johan Neyts[3], Xavier de Lamballerie[1], Antoine Nougairède[1]

Affiliations:

[1] Unité des Virus Émergents (UVE: Aix-Marseille Univ-IRD 190-Inserm 1207), Marseille, France

[2] KU Leuven Department of Microbiology, Immunology and Transplantation, Laboratory of Clinical and Epidemiological Virology, Rega Institute, Leuven, Belgium

[3] KU Leuven Department of Microbiology, Immunology and Transplantation, Laboratory of Virology and Chemotherapy, Rega Institute, Leuven, Belgium

* These authors contributed equally to this article.

Corresponding author: Antoine Nougairède (antoine.nougairede@univ-amu.fr)

Key words: SARS-CoV-2; B.1.1.7; B.1.351; 20I/501Y.V1; 20H/501Y.V2; hamster model; transmission; replicative fitness; host response

Words count: 3 260

Abstract

Late 2020, SARS-CoV-2 20I/501Y.V1 variant from lineage B.1.1.7 emerged in United Kingdom and gradually replaced the D614G strains initially involved in the global spread of the pandemic. In this study, we used a Syrian hamster model to compare a clinical strain of 20I/501Y.V1 variant with an ancestral D614G strain. The 20I/501Y.V1 variant succeeded to infect animals and to induce a pathology that mimics COVID-19. However, both strains induced replicated to almost the same level and induced a comparable disease and immune response. A slight fitness advantage was noted for the D614G strain during competition and transmission experiments. These data do not corroborate the current epidemiological situation observed in humans nor recent reports that showed a more rapid replication of the 20I/501Y.V1 variant in human reconstituted bronchial epithelium.

Introduction

The genetic evolution of the severe acute respiratory syndrome coronavirus 2 (SARS-CoV-2) virus is a constant concern for medical and scientific communities. From January 2020, viruses carrying the spike D614G mutation emerged in several countries [1–3]. In June, D614G SARS-CoV-2 lineage B.1 became the dominant form of circulating virus worldwide and replaced the initial SARS-CoV-2 strains related to the outbreak in Wuhan, China. Experimental data from human lung epithelium and animal models revealed that the D614G substitution increased virus infectivity and transmissibility as compared to an original D614 strain [4]. However, it seems that this D614G variant does not cause more severe clinical disease. In late 2020, three SARS-CoV-2 variants sharing the N501Y spike mutation located in the receptor binding motif (RBM) emerged almost simultaneously in the United Kingdom (20I/501Y.V1 variant from lineage B.1.1.7 ; initially named VOC 202012/01) [5], in South Africa (501Y.V2 variant from lineage B.1.351) [6] and in Brazil (P.1 variant from lineage B.1.1.28.1) [7]. As previously observed with the D614G variant, the 20I/501Y.V1 variant spread rapidly and became dominant in United Kingdom in December 2020, and in many other European and non-European countries from February 2021 onwards [8]. This similar evolution pattern seems to be associated with an improved affinity of the viral spike protein for the human angiotensin-converting enzyme 2 (ACE2) receptor [9,10]. The 20I/501Y.V1 variant harbors 8 additional spike mutations, including substitutions and deletions, compared to D614G circulating strains. At this stage, there are few data regarding the 20I/501Y.V1 variant pathogenicity and its ability to spread more easily [11,12]. Recent studies also revealed that the active circulation of the 20I/501Y.V1 variant may not impact the risk of reinfection, the efficiency of vaccine campaigns and antibody therapies remains also unknown [13–15]. We recently described the fitness advantage of 20I/501Y.V1 variant using a model of reconstituted bronchial human epithelium [16]. In the present work, we compared the

phenotype of the 20I/501Y.V1 variant (hCoV-103 19/Belgium/rega-12211513/2020 strain) with that of a D614G strain (Germany/BavPat1/2020 strain) in the Syrian hamster (*Mesocricetus auratus*) model. The study includes comparison of viral replication kinetics, transmissibility, clinical course of the disease and immunological response.

Materials and methods

Cells and viruses

VeroE6 cells (ATCC CRL-1586) were grown at 37°C with 5% CO_2 in minimal essential medium (MEM) supplemented with 1% non-essential amino acids, 1% Penicillin/Streptomycin and 7% of heat-inactivated fetal bovine serum (FBS) (all from ThermoFisher Scientific). VeroE6/TMPRSS2 cells (NIBSC 100978) were grown in the same medium supplemented with G-418 (ThermoFisher Scientific).

All experiments with infectious virus were conducted in biosafety level (BSL) 3 laboratory. SARS-CoV-2 strain BavPat1 (BavPat D614G), supplied through European Virus Archive GLOBAL (https://www.european-virus-archive.com/), was kindly provided by Christian Drosten (Berlin, Germany). SARS-CoV-2 20I/501Y.V1 hCoV104 19/Belgium/rega-12211513/2020 strain (EPI_ISL_791333, 2020-12-21), was kindly provided by Piet Maes (Leuven, Belgium) and Johann Neyts (Leuven, Belgium). SARS CoV-2 'South African' 20H/501Y.V2 variant (lineage B 1.351), strain UVE/SARS-CoV-2/2021/FR/1299-ex SA was isolated in France in 2021. This strain is available through EVA GLOBAL at https://www.european-virus-archive.com/virus/sars-cov-2-uvesars-cov-22021fr1299-ex-sa-lineage-b-1351. All virus stocks were prepared using VeroE6 (BavPat D614G and 20I/501Y.V1 strains) or VeroE6/TMPRSS2 cells (20H/501Y.V2) and were characterized (full-genome sequencing).

In vivo experiments

Following approval by the local ethical committee (C2EA—14) and the French 'Ministère de l'Enseignement Supérieur, de la Recherche et de l'Innovation' (APAFIS#23975), *in vivo* experiments were performed in accordance with the French national guidelines and the European legislation covering the use of animals for scientific purposes.

For each experiment, groups of three-week-old female Syrian hamsters (Janvier Labs) were intranasally infected under general anesthesia (isofluorane) with 50µL containing $2x10^3$ or 40 $TCID_{50}$ of virus diluted in 0.9% sodium chloride solution. With the exception of transmission experiments, all experiments were performed twice (two independent experiments with groups of 6 animals). Pooled data from both experiments (12 animals) were presented. Groups of 12 animals were used for transmission experiments. Animals were maintained in ISOcage P - Bioexclusion System (Techniplast) with unlimited access to water/food and 14h/10h light/dark cycle. Animals were monitored and weighed daily throughout the duration of the study to detect the appearance of any clinical signs of illness/suffering. Nasal washes were performed under general anesthesia (isoflurane). Blood and organs were collected after euthanasia (cervical dislocation; realized under general anesthesia (isofluorane)).

Organ collection

Nasal washes were performed with 150µl 0.9% sodium chloride solution which was transferred into 1.5mL tubes containing 0.5mL of 0.9% sodium chloride solution, then centrifuged at 16,200g for 10 minutes and stored at -80°C. Lung, gut and blood samples were collected immediately after the time of sacrifice. Left pulmonary lobes were washed in 10mL of 0.9% sodium chloride solution, blotted with filter paper, weighed and then transferred into 2mL tubes containing 1mL of 0.9% sodium chloride solution and 3mm glass beads. Guts (part of small and large bowels) were empty of their alimentary bolus, weighed and then transferred into 2mL tubes containing 1mL of 0.9% sodium chloride solution and 3mm glass beads. Left

pulmonary lobes and guts were crushed using a Tissue Lyser machine (Retsch MM400) for 20min at 30 cycles/s and then centrifuged 10min at 16,200g. Supernatant media were transferred into 1.5mL tubes, centrifuged 10 min at 16,200g and stored at -80°C. One milliliter of blood was harvested in a 2mL tube containing 100µL of 0.5M EDTA (ThermoFischer Scientific) and then centrifuged 10 min at 16,200g to obtain plasma. Serum samples were collected from blood harvested in a 2mL tube incubate 15 min at room temperature and then centrifuged 10 min at 16,200g. Blood-derived samples were stored at -80°C. To assess the expression level of seven cytokines in lungs, right apical lobes were collected into 2mL tubes containing 0.75mL of Qiazol lysis reagent (Qiagen) and 3mm glass beads. They were then crushed using a Tissue Lyser machine (Retsch MM400) for 10min at 30 cycles/s and stored at -80°C.

$TCID_{50}$ assay

Virus titration was performed using 96-well culture plates containing confluent VeroE6 cells inoculated with 150µL per well of four-fold dilutions of samples (dilution with medium supplemented with 2.5% FBS). After 6 days of incubation (37°C, 5% CO_2) the absence or presence of cytopathic effect in each well was read and infectious titers were estimated using the Reed & Muench method[17].

Molecular biology

For viral quantification, nucleic acids from each sample were extracted using QIAamp 96 DNA kit and Qiacube HT robot (both from Qiagen). Viral RNA yields were measured using a RT-qPCR assay targeting the *rdrp* gene as previously described[18].

To analyze samples from competition and transmission experiments (ie. with animal infected with a mix of both viruses), we used two specific RT-qPCR assays targeting the NSP6 coding region (each specifically detecting one of the competing viruses) to determine the proportion

of each viral genome. Prior to PCR amplification, RNA extraction was performed as described above. RT-qPCR were performed with SuperScript III Platinum One-Step qRT-PCR kit (SuperScript™ III Platinum™ One-Step qRT-PCR kit, universal Invitrogen) using 2.5µL of nucleic acid extract and 7.5µL of RT-qPCR reagent mix. Using standard fast cycling parameters, i.e., 50°C for 15min, 95°C for, and 40 amplification cycles (15 sec at 95°C followed by 45 sec at 55°C). RT-qPCR reactions were performed on QuantStudio 12K Flex Real-Time PCR System (Applied Biosystems) and analyzed on QuantStudio 12K Flex Applied Biosystems software v1.2.3. Viral RNA quantities were calculated using serial dilutions of T7-generated synthetic RNA standards. Primers and probes sequences were: Fwd: 5’-CATGGTTGGATATGGTTG-3’; Rev: 5’-GATGCATACATAACACAG-3’; Probe that specifically detect the BavPat D614G virus: 5'-FAM-GTCTGGTTTTAA-BHQ1-3'; Probe that specifically detect the 201/501YV.1 variant: 5'-VIC-TAGTTTGAAGCT-BHQ1-3'.

To assess the expression level of seven cytokines in lungs, 150µL of chloroform was added to crush lung samples. After, centrifugation (15min at 4°C and 12000g), 300µL of the aqueous phase was used for RNA extraction using EZ1 RNA tissue mini kit and EZ1 advanced XL robot (both from Qiagen). Quantitative RT-qPCR were performed using primers previously described by Dias de Melo *et al*[19] using QuantiNova SYBR® Green RT-PCR Kit (Qiagen) according to the manufacturer instructions. RT-qPCR reactions were performed on QuantStudio 12K Flex Real-Time PCR System (Applied Biosystems) and analyzed on QuantStudio 12K Flex Applied Biosystems software v1.2.3. All cytokine mRNA quantifications were performed using serial dilutions of synthetic standards. Data were normalized to γ−actin reference gene relative expression[19].

Seroneutralization assay

One day prior to infection, 5×10^4 VeroE6/TMPRSS2 cells per well were seeded in 100µL assay medium (containing 2.5% FBS) in 96 well culture plates. The next day, 25µL of a virus mix diluted in medium was added to the wells. The amount of virus working stock used was calibrated prior to the assay, based on a replication kinetics, so that the viral replication was still in the exponential growth phase for the readout as previously described[20,21]. This corresponds here to a MOI of 0.002. Then six 2-fold serial dilutions of hamster sera starting at 1/10 were added to the cells (25µL/well, in assay medium) in duplicate. In addition, three 2-fold dilutions of a negative serum (from uninfected animals) starting at 1/10 were added to the plate to assess virus replication in presence of hamster serum (called 'negative serum' below). Four 'virus control' wells were supplemented with 25µL of assay medium to verify viral replication without serum. Plates were first incubated 15min at room temperature and then 2 days at 37°C prior to quantification of the viral genome by real-time RT-qPCR as previously described[22]. Briefly, nucleic acid from 100µL of cell supernatant were extracted using QIAamp 96 DNA kit and Qiacube HT robot (both from Qiagen). Viral RNA was quantified by real-time RT-qPCR (GoTaq 1 step RT-qPCR kit, Promega). Quantification was provided by serial dilutions of an appropriate T7-generated synthetic RNA standard. RT-qPCR reactions were performed on QuantStudio 12K Flex Real-Time PCR System (Applied Biosystems) and analyzed using QuantStudio 12K Flex Applied Biosystems software v1.2.3. Primers and probe sequences, which target SARS-CoV-2 N gene, were: Fw: 5'-GGCCGCAAATTGCACAAT-3'; Rev : 5'-CCAATGCGCGACATTCC-3'; Probe: 5'-FAM-CCCCCAGCGCTTCAGCGTTCT-BHQ1-3'. Percentage of viral inhibition was calculated as follows: 100* (mean quantity for negative serum- sample quantity)/mean quantity for negative serum. The 90% and 99% inhibition dilution factor were determined using logarithmic interpolation as previously described[20,22].

Graphical representations and statistical analysis

Timelines (Figure 1.a and 2.a) were created on *biorender.com*. Graphical representations and statistical analysis were performed using GraphPad Prism 7 software (GrapPad software). For each group of data we applied the Shapiro-Wilk normality test. Then a two-by-two comparison of groups was performed using either an unpaired t test with or without a Welch correction if the variance did not assume an equal distribution (according to a Fisher test) or a Mann-Whitney test if the distribution was non-Gaussian.

Results

First, to detect modifications of the clinical course of the disease following infection with the 20I/501Y.V1 variant, groups of 12 three-week-old female Syrian hamsters were intranasally infected with 50µl containing $2x10^3 TCID_{50}$ of 20I/501Y.V1 or BavPat D614G strain (Figure 1.a). Follow-up of these animals until 7 days post-infection (dpi) showed with both strains a lack of weight gain compared to mock-infected group. Normalized weights (i.e. % of initial weights) of animals infected with 20I/501Y.V1 variant were significantly higher than those of BavPat D614G group at 3, 4 and 5 dpi (p values between 0.0403 and 0.0007)(Figure 1.b). However, this difference seems to be the result of a delayed onset of disease for 20I/501Y.V1 variant since significant difference of normalized weights compared to mock-infected group began at 2 dpi for animals infected with BavPat D614G strain and at 3 dpi for those infected with the 20I/501Y.V1 variant.

Second, to further investigate viral replication, groups of 12 three-week-old female Syrian hamsters were intranasally infected with 50µl containing $2x10^3 TCID_{50}$ of each viral strain and several tissues were collected at different time points (Figure 1.a).

Viral RNA quantification was performed using a RT-qPCR assay (i) in lung and nasal wash samples collected at 2, 4 and 7 dpi, and (ii) in blood and gut samples collected at 2 and 4 dpi. Infectious titers were determined using a $TCID_{50}$ assay in lungs and nasal washes at 2 and 4

dpi. Overall, the results indicated that the 20I/501Y.V1 variant properly replicate in the hamster gut and respiratory tract. However, higher viral RNA yields were found in all samples from animals infected with BavPat D614G strain (difference ranged from 0.085 to 0.801 log_{10}). This difference was significant in lung and gut at any time point (p values ranging between 0.0332 and 0.0084) (Figure 1.c.d.e). Results of plasma did not show any significant difference (Supplemental Figure 1.a). A similar pattern was observed when assessing infectious viral loads using a $TCID_{50}$ assay (differences ranged from 0.0343 to 0.389 log_{10}) but no significant difference was found (Figure 1.f.g).

To detect more subtle differences of viral replication *in vivo*, we performed competitions experiments as previously described [9,23]. Groups of 12 animals were simultaneously infected intranasally with 50µl containing 50% (10^3 $TCID_{50}$) of each viral strain. Lungs, nasal washes and plasma were collected at 2 and 4 dpi (Figure 1.a). Using two specific RT-qPCR systems, we estimated in all samples the proportion of each viral genome in the viral population (expressed as BavPat D614G/20I/501Y.V1 ratios in Figure 1.h.i). Once again, results revealed that BavPat D614G strain seems to replicate a somewhat more efficiently and supplants progressively the 20I/501Y.V1 variant. Indeed, BavPat D614G/ 20I/501Y.V1 estimated ratios at 4dpi were significantly higher than those at 2 dpi in nasal washes (p=0.0001). Moreover, ratios at 4 dpi in nasal washes were also significantly higher than those in the infecting inoculum (p=0.022) (Figure 1.i). By contrast, no significant difference was found in lungs (Figure 1.h) and plasma (supplemental Figure 1.b).

To obtain a clearer picture, we compared the transmissibility of both strains in a last *in vivo* experiment. To increase the sensitivity of the procedure, groups of 12 animals were simultaneously infected intranasally with 50µl containing a low dose of each viral strain (20 $TCID_{50}$). These animals, called ‘donors’, firstly housed individually, were co-housed at 2 dpi with an uninfected animal, called ‘contact’, during a period of 6 hours in a new cage. Then,

donors returned in their initial cages and were sacrificed at 3 dpi. Contact animals were sacrificed at 3 days post-contact (Figure 2.a). Using the two specific RT-qPCR systems used for competition experiments, we estimated in all samples (nasal washes and lungs) the proportion of each viral genome in the viral population (Figure 2.b). Data from lungs of donors showed for two animals, an equivalent proportion of both viruses (from 40% to 60% of each strain); for five animal, a majority (>60%) of BavPat D614G virus; and for the five remaining animals, a majority (>60%) of 20I/501Y.V1 virus. However, we did not find the same distribution in nasal washes in which we observed: for eight animals, an equivalent proportion of both viruses; for four animal, a majority of BavPat D614G virus; and for no animal, a majority of 20I/501Y.V1 virus. Consistently with this observation, we found a large majority (>75%) of BavPat D614G virus in lungs and nasal washes of eight contacts, and only two and one animals exhibited a large majority (>75%) of 20I/501Y.V1 virus in lungs and nasal washes respectively (Figure 2.b). When analyzing the data from each pair of animals, we observed an increase of the proportion of Bavpat D614G virus between the nasal wash of the donor and lungs of the contact in almost all cases (10/12).

Altogether, our results suggest that the replication of both strains was highly comparable in hamsters. Nonetheless, using a more sensitive method, we observed that the 20I/501Y.V1 variant is outcompeted by the BavPat D614G strain; it results in an advantage for the BavPat D614G strain during transmission experiments. Notably, such results are not in line with experimental data *ex vivo* (human epithelial cultures grown at the air liquid interface) and with epidemiological observations.

We then compared transcriptional early immune signatures in lungs from animals sacrificed at 4 dpi following intranasal infection with 50µl containing $2x10^3 TCID_{50}$ of 20I/501Y.V1 or BavPat D614G strain. The expression level of seven cytokines (Interferon-γ, TNF-α, IL-6, IL-10, IL-1β, Cxcl-10, Ccl5) was quantified using RT-qPCR assays (Supplemental Figure 2;

expressed as mRNA copies/γ-actin copies). Infection by both viral strains induced an important increase of CXCL10, CCL5, IFNγ, Il-6 and Il-10 expression levels ($p<0.0001$) and a moderate increase of Il-1β ($p=0.0014$ for BavPat D614G and $p=0.0281$ for 20I/501Y.V1) and TNFα ($p=0.0389$ for BavPat D614G and $p=0.0350$ for 20I/501Y.V1) expressions levels to mock-infected animals (Supplemental Figure 2). Comparison between animals infected with 20I/501Y.V1 and BavPat D614G strains did not show any significant differences of cytokines expression levels. This suggests that the early immune response induced by both viral strains is similar, in line with a recent study that did not present major differences except an upregulation of Il-6, Il-10 and IFNγ with animals infected by 20I/501Y.V1 variant [24].

Finally, we used sera collected at 7 dpi following intranasal infection with 50µl containing $2x10^3 TCID_{50}$ of 20I/501Y.V1 (n=4) or BavPat D614G (n=4) (Figure 1.a) strain to assess the level of protection against three circulating strains of SARS-CoV-2: the BavPat D614G strain, the 20I/501Y.V1 variant and a 'South-African' 20H/501Y.V2 (lineage B 1.351) variant. Sera were tested for the presence of antibodies using a 90-99% viral RNA Yield Reduction Neutralization Test (YRNT90/YRNT99) (Figure 1.j.k). Overall, results showed that animals infected with 20I/501Y.V1 or BavPat D614G strains produced similar levels of neutralization antibodies against these strains. However, all infected animals produced lower neutralization titers against the 20H/501Y.V2 variant. This difference is significant with all animals when considering YRNT90 titers (p values between 0.001 and 0.045), and significant only with animals infected with 20I/501Y.V1 variant when considering YRNT99 titers ($p < 0.048$) (Supplemental Table 1). This suggests an effective cross-immunity between 20I/501Y.V1 and BavPat D614G, but a reduced cross-protection against the 20H/501Y.V2 variant. These data indicate that only an active circulation of 20H/501Y.V2 variant might increase the risk of

reinfection or failure of vaccination campaigns. This is in accordance with recently reported epidemiological observation [25–29].

Discussion

Our results show that the 20I/501Y.V1 variant induces a pathology that mimics human SARS-CoV-2 infection in the hamster model and can be used for preclinical analysis of vaccines and therapeutic agents. These data corroborate those of a recent study in which the same strains, a similar hamster model but higher virus inocula (10^5 $TCID_{50}$) were used [24]. Since its emergence in late 2020 in Europe, the 20I/501Y.V1 variant spread across several continents and became the majority circulating strain in many countries. Moreover, data from reconstituted human airway epithelia also showed a strong replicative fitness advantage for 20I/501Y.V1 variant [16]. Notably, our findings in the hamster model are not in line with these observations. Altogether, this suggests that the hamster model may possibly not be the best model to detect weak fitness or transmissibility differences between clinical strains of SARS-CoV-2. Other animal models such as the ferret (*Mustela putorius furo*) model that is already employed to study the pathogenicity and transmissibility of other human respiratory viruses, could be valuable tools in that case. Nevertheless, in a recent study that used engineered rescued viruses derived from the USA_WA1/2020 strain, the hamster model appeared useful to detect weak fitness advantages and an increases in transmissibility of viruses that carry the N501Y and A570D spike mutations. However, the role of other mutations located in other parts of the genome of the 20I/501Y.V1 variant [more than twenty when compared to strains isolated in January-February 2020], was obviously not taken into account using this reverse genetics-based approach.

Acknowledgments

This work was supported by the European Union's Horizon 2020 Research and Innovation Programme under grant agreements no. 653316 (European Virus Archive goes global project: http://www.european-virus-archive.com/). We also thank Noémie Courtin for her technical support.

Declaration of conflicting interests

Authors declare that there is no conflict of interest

References

[1] Volz E, Hill V, McCrone JT, et al. Evaluating the Effects of SARS-CoV-2 Spike Mutation D614G on Transmissibility and Pathogenicity. Cell. 2021;184:64-75.e11.

[2] Yurkovetskiy L, Wang X, Pascal KE, et al. Structural and Functional Analysis of the D614G SARS-CoV-2 Spike Protein Variant. Cell. 2020;183:739-751.e8.

[3] Korber B, Fischer WM, Gnanakaran S, et al. Tracking Changes in SARS-CoV-2 Spike: Evidence that D614G Increases Infectivity of the COVID-19 Virus. Cell. 2020;182:812-827.e19.

[4] Plante JA, Liu Y, Liu J, et al. Spike mutation D614G alters SARS-CoV-2 fitness. Nature. 2020;1–6.

[5] du Plessis L, McCrone JT, Zarebski AE, et al. Establishment and lineage dynamics of the SARS-CoV-2 epidemic in the UK. Science. 2021;371:708–712.

[6] National Center for Immunization and Respiratory Diseases (U.S.). Division of Viral Diseases., editor. Emerging SARS-CoV-2 variants. 2021; Available from: https://stacks.cdc.gov/view/cdc/100655.

[7] Sabino EC, Buss LF, Carvalho MPS, et al. Resurgence of COVID-19 in Manaus, Brazil, despite high seroprevalence. Lancet Lond Engl. 2021;397:452–455.

[8] CoVariants [Internet]. [cited 2021 Apr 15]. Available from: https://covariants.org/per-country.

[9] Liu Y, Liu J, Plante KS, et al. The N501Y spike substitution enhances SARS-CoV-2 transmission. bioRxiv. 2021;2021.03.08.434499.

[10] Zahradník J, Marciano S, Shemesh M, et al. SARS-CoV-2 RBD *in vitro* evolution follows contagious mutation spread, yet generates an able infection inhibitor [Internet].

Biochemistry; 2021 [cited 2021 Mar 24]. Available from: http://biorxiv.org/lookup/doi/10.1101/2021.01.06.425392.

[11] Davies NG, Jarvis CI, Edmunds WJ, et al. Increased mortality in community-tested cases of SARS-CoV-2 lineage B.1.1.7. Nature. 2021;1–5.

[12] Zhao S, Lou J, Cao L, et al. Quantifying the transmission advantage associated with N501Y substitution of SARS-CoV-2 in the UK: an early data-driven analysis. J Travel Med [Internet]. 2021 [cited 2021 Apr 15];28. Available from: https://doi.org/10.1093/jtm/taab011.

[13] Shen X, Tang H, McDanal C, et al. SARS-CoV-2 variant B.1.1.7 is susceptible to neutralizing antibodies elicited by ancestral Spike vaccines. Cell Host Microbe [Internet]. 2021 [cited 2021 Mar 9];0. Available from: https://www.cell.com/cell-host-microbe/abstract/S1931-3128(21)00102-5.

[14] Planas D, Bruel T, Grzelak L, et al. Sensitivity of infectious SARS-CoV-2 B.1.1.7 and B.1.351 variants to neutralizing antibodies. Nat Med. 2021;1–8.

[15] Chen RE, Zhang X, Case JB, et al. Resistance of SARS-CoV-2 variants to neutralization by monoclonal and serum-derived polyclonal antibodies. Nat Med. 2021;1–10.

[16] Touret F, Luciani L, Baronti C, et al. Replicative fitness SARS-CoV-2 20I/501Y.V1 variant in a human reconstituted bronchial epithelium. bioRxiv. 2021;2021.03.22.436427.

[17] REED LJ, MUENCH H. A SIMPLE METHOD OF ESTIMATING FIFTY PER CENT ENDPOINTS12. Am J Epidemiol. 1938;27:493–497.

[18] Driouich J-S, Cochin M, Lingas G, et al. Favipiravir antiviral efficacy against SARS-CoV-2 in a hamster model. Nat Commun. 2021;12:1735.

[19] de Melo GD, Lazarini F, Larrous F, et al. Anti-COVID-19 efficacy of ivermectin in the golden hamster [Internet]. Immunology; 2020 [cited 2021 Mar 9]. Available from: http://biorxiv.org/lookup/doi/10.1101/2020.11.21.392639.

[20] Touret F, Baronti C, Goethals O, et al. Phylogenetically based establishment of a dengue virus panel, representing all available genotypes, as a tool in dengue drug discovery. Antiviral Res. 2019;168:109–113.

[21] Delang L, Li C, Tas A, et al. The viral capping enzyme nsP1: a novel target for the inhibition of chikungunya virus infection. Sci Rep. 2016;6:31819.

[22] Touret F, Gilles M, Barral K, et al. In vitro screening of a FDA approved chemical library reveals potential inhibitors of SARS-CoV-2 replication. Sci Rep. 2020;10:13093.

[23] Fabritus L de, Nougairède A, Aubry F, et al. Attenuation of Tick-Borne Encephalitis Virus Using Large-Scale Random Codon Re-encoding. PLOS Pathog. 2015;11:e1004738.

[24] Abdelnabi R, Boudewijns R, Foo CS, et al. Comparative infectivity and pathogenesis of emerging SARS-CoV-2 variants in Syrian hamsters. bioRxiv. 2021;2021.02.26.433062.

[25] Nonaka CKV, Franco MM, Gräf T, et al. Genomic Evidence of a SARS-CoV-2 Reinfection Case with E484K Spike Mutation in Brazil. 2021 [cited 2021 Mar 31]; Available from: https://www.preprints.org/manuscript/202101.0132/v2.

[26] Nonaka CKV, Franco MM, Gräf T, et al. Genomic Evidence of SARS-CoV-2 Reinfection Involving E484K Spike Mutation, Brazil. Emerg Infect Dis [Internet]. 2021 [cited 2021 Mar 31];27. Available from: https://wwwnc.cdc.gov/eid/article/27/5/21-0191_article.htm.

[27] Jangra S, Ye C, Rathnasinghe R, et al. The E484K mutation in the SARS-CoV-2 spike protein reduces but does not abolish neutralizing activity of human convalescent and post-vaccination sera. medRxiv. 2021;2021.01.26.21250543.

[28] Zucman N, Uhel F, Descamps D, et al. Severe reinfection with South African SARS-CoV-2 variant 501Y.V2: A case report. Clin Infect Dis Off Publ Infect Dis Soc Am [Internet]. 2021 [cited 2021 Mar 31]; Available from: https://www.ncbi.nlm.nih.gov/pmc/articles/PMC7929064/.

[29] Graham MS, Sudre CH, May A, et al. The effect of SARS-CoV-2 variant B.1.1.7 on symptomatology, re-infection and transmissibility. medRxiv. 2021;2021.01.28.21250680.

Figures and Legends

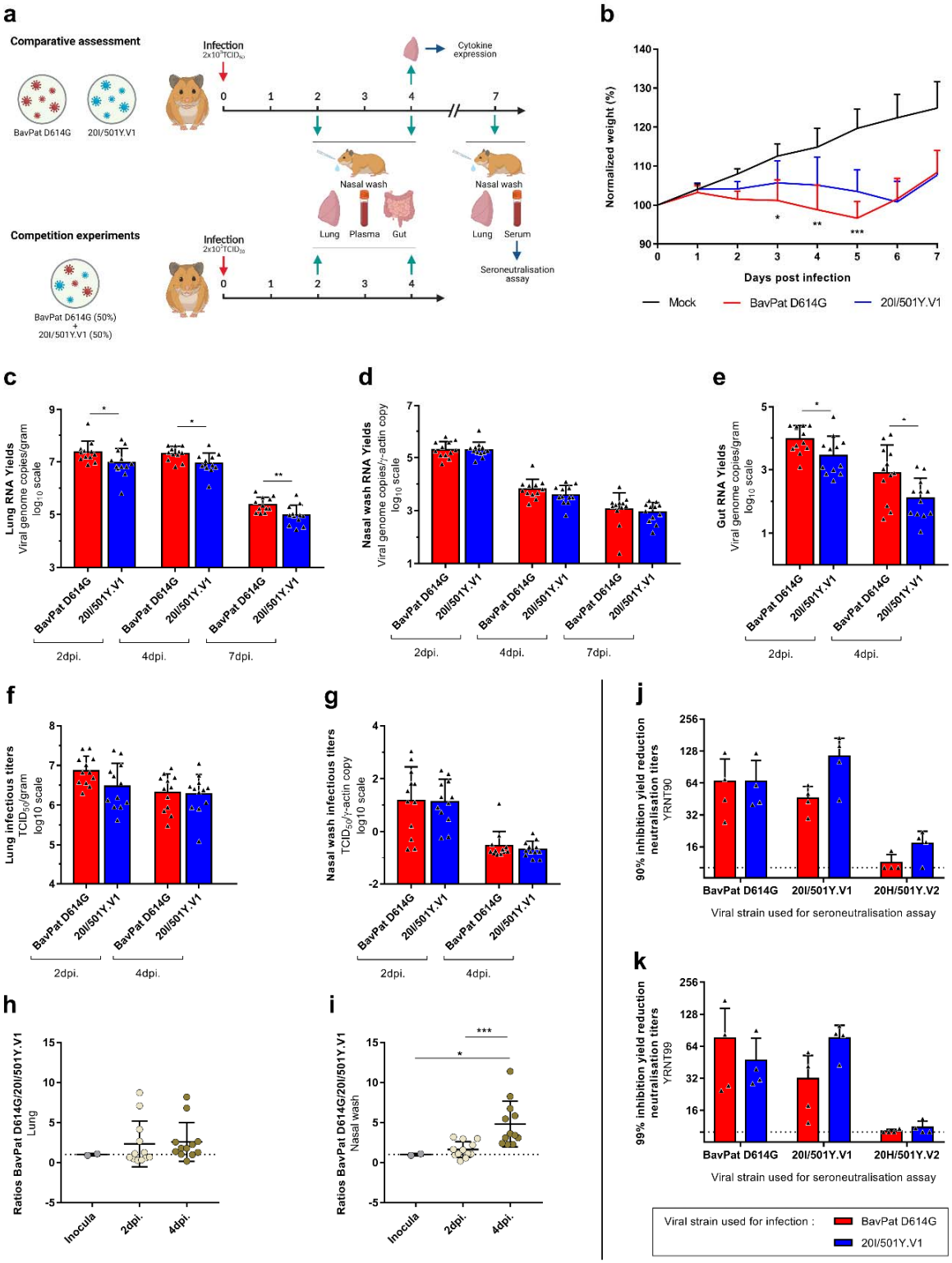
a
Comparative assessment
BavPat D614G
20I/501Y.V1
Infection
Cytokine expression
Nasal wash
Lung
Plasma
Gut
Serum
Seroneutralisation assay
Competition experiments
BavPat D614G (50%) + 20I/501Y.V1 (50%)
b
Normalized weight (%)
Days post infection
Mock
BavPat D614G
20I/501Y.V1
c
Lung RNA Yields
Viral genome copies/gram log10 scale
d
Nasal wash RNA Yields
Viral genome copies/γ-actin copy log10 scale
e
Gut RNA Yields
Viral genome copies/gram log10 scale
2dpi.
4dpi.
7dpi.
f
Lung infectious titers
TCID50/gram log10 scale
g
Nasal wash infectious titers
TCID50/γ-actin copy log10 scale
h
Ratios BavPat D614G/20I/501Y.V1 Lung
Inocula
i
Ratios BavPat D614G/20I/501Y.V1 Nasal wash
j
90% inhibition yield reduction neutralisation titers YRNT90
20H/501Y.V2
Viral strain used for seroneutralisation assay
k
99% inhibition yield reduction neutralisation titers YRNT99
Viral strain used for infection :

Figure 1

Figure 1: Clinical follow-up, viral replication in Syrian hamsters and seroneutralization tests. (a) Experimental timeline. Groups of 12 hamsters were intranasally infected with $2x10^3$ $TCID_{50}$ of 20I/501Y.V1 or BavPat D614G strain for comparative assessment, or with a mix (1:1) of both viral strains for competition experiment (10^3 $TCID_{50}$ of each). (b) Comparative clinical follow-up. Weights are expressed as normalized weights (i.e. % of initial weight). ***, ** and * symbols indicate that normalized weights for the 20I/501Y.V1 group are significantly higher than those of the BavPat D614G group with a p-value ranging between 0.0001-0.001, 0.001–0.01, and 0.01–0.05, respectively (Two-way ANOVA test with Tukey's post-hoc analysis). (c-e) Comparative assessment of viral RNA yields in lungs (c), nasal washes (d) and guts (e), measured using a RT-qPCR assay. ** and * symbols indicate that viral RNA yields for the 20I/501Y.V1 group are significantly lower than those of the BavPat D614G group with a p-value ranging between 0.001–0.01, and 0.01–0.05, respectively (Mann-Whitney and Unpaired t tests). (f-g) Comparative assessment of infectious titers in lungs (f) and nasal washes (g), measured using a $TCID_{50}$ assay. (h-i) Competition experiments. Two specific RT-qPCR assays were used to measure the quantity of each virus in lungs (h) and nasal washes (i). Results are expressed as [BavPat D614G/ 20I/501Y.V1] ratios. *** and * symbols indicate that ratios at 4 dpi are higher than those at 2 dpi or in inocula with a p-value ranging between 0.0001-0.001 and 0.01–0.05, respectively (Mann-Whitney tests). (j-k) Seroneutralization tests performed with sera from animals sacrificed at 7 dpi. 90% (j) and 99% (k) Yield Reduction Neutralization Titers (90-99YRNT) were determined against three strains of SAR-CoV-2: BavPat D614G, 20I/501Y.V1 and 20H/501Y.V2. Results from statistical analysis are presented in Supplemental Table 1. (b-k) Data represent mean ± SD.

Figure 2

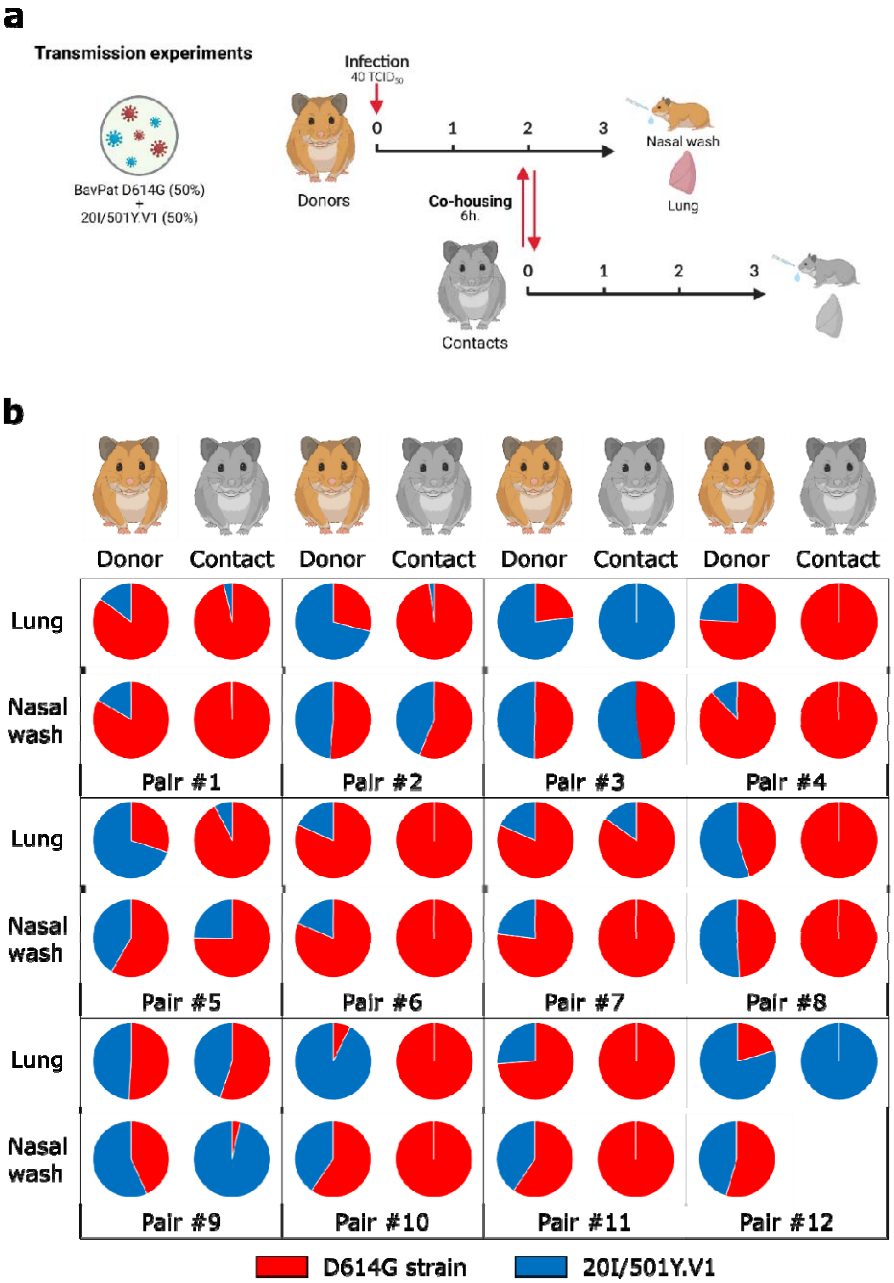

Figure 2: Transmission experiments. (a) Experimental timeline. A group of 12 hamsters, named donors, was intranasally infected with a mix (1:1) of both viral strains for competition experiment (20 $TCID_{50}$ of each). At 2 dpi, each donor was co-housed with a contact animal during a period of 6 hours. Donors and contacts were sacrificed at 3dpi and at 3 days post-contact respectively. (b) Graphical representation of the proportion of each virus found in lungs and nasal washes for each pair of animals. Two specific RT-qPCR assays were used to measure the quantity of each virus. The grey circle means that no viral RNA was detected in this nasal wash.

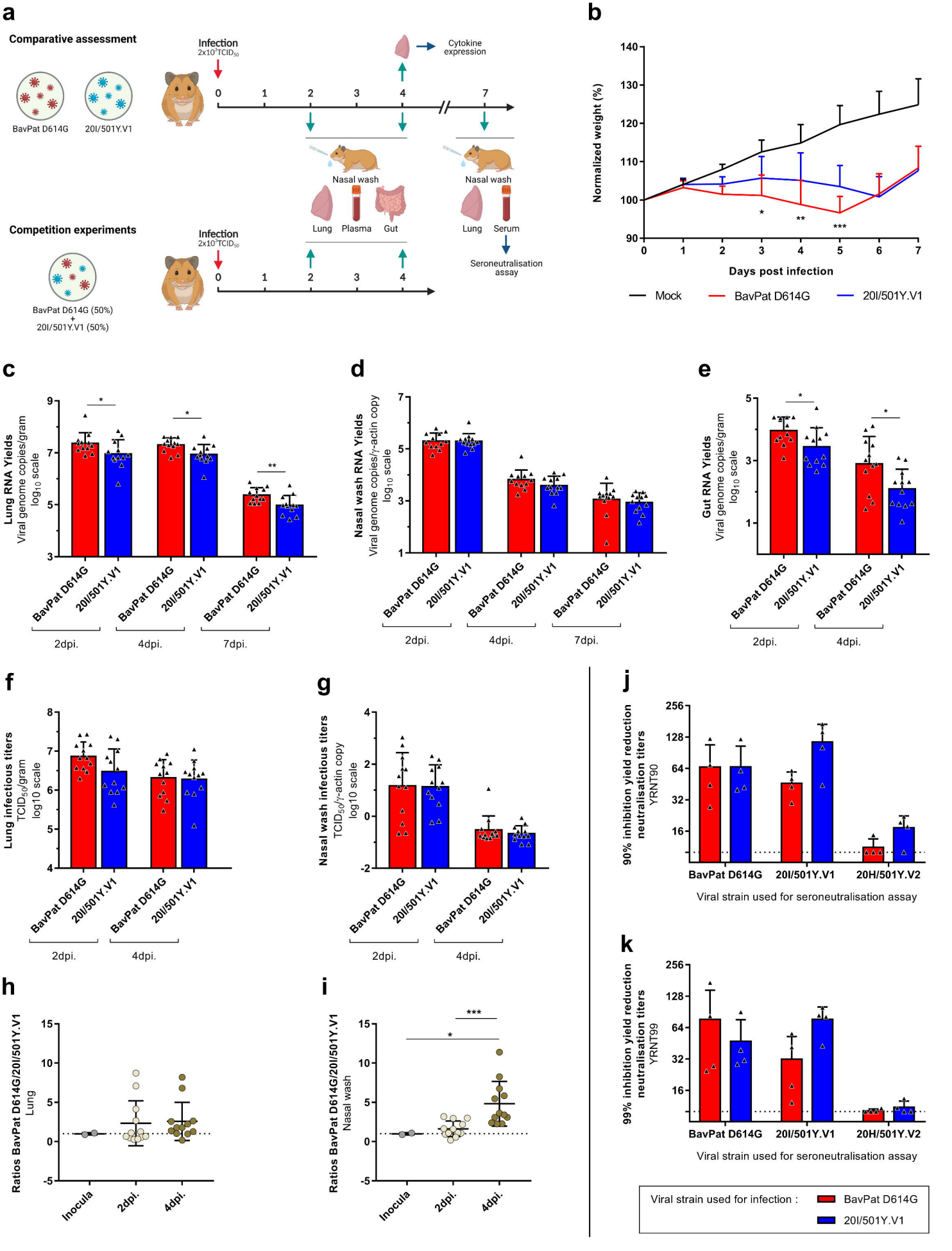
a
Comparative assessment
BavPat D614G
20I/501Y.V1
Infection
2x10⁴TCID50
Cytokine expression
Nasal wash
Lung
Plasma
Gut
Serum
Seroneutralisation assay
Competition experiments
BavPat D614G (50%)
+
20I/501Y.V1 (50%)
b
Normalized weight (%)
Days post infection
Mock
BavPat D614G
20I/501Y.V1
c
Lung RNA Yields
Viral genome copies/gram
log10 scale
2dpi.
4dpi.
7dpi.
d
Nasal wash RNA Yields
Viral genome copies/γ-actin copy
log10 scale
e
Gut RNA Yields
f
Lung infectious titers
TCID50/gram
log10 scale
g
Nasal wash infectious titers
TCID50/γ-actin copy
h
Ratios BavPat D614G/20I/501Y.V1
Lung
Inocula
i
Nasal wash
j
90% inhibition yield reduction neutralisation titers
YRNT90
20H/501Y.V2
Viral strain used for seroneutralisation assay
k
99% inhibition yield reduction neutralisation titers
YRNT99
Viral strain used for infection :

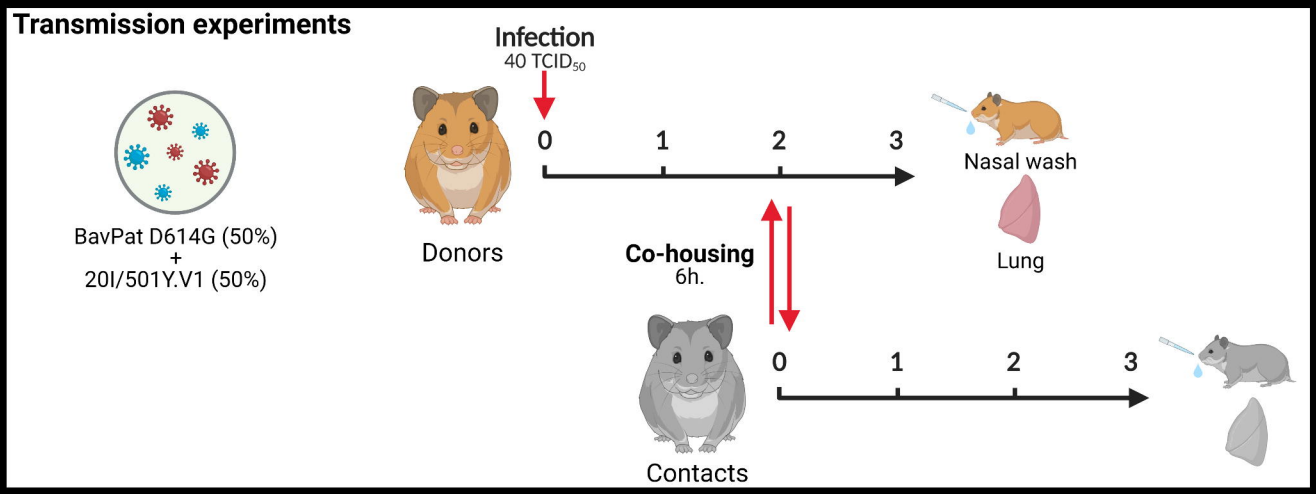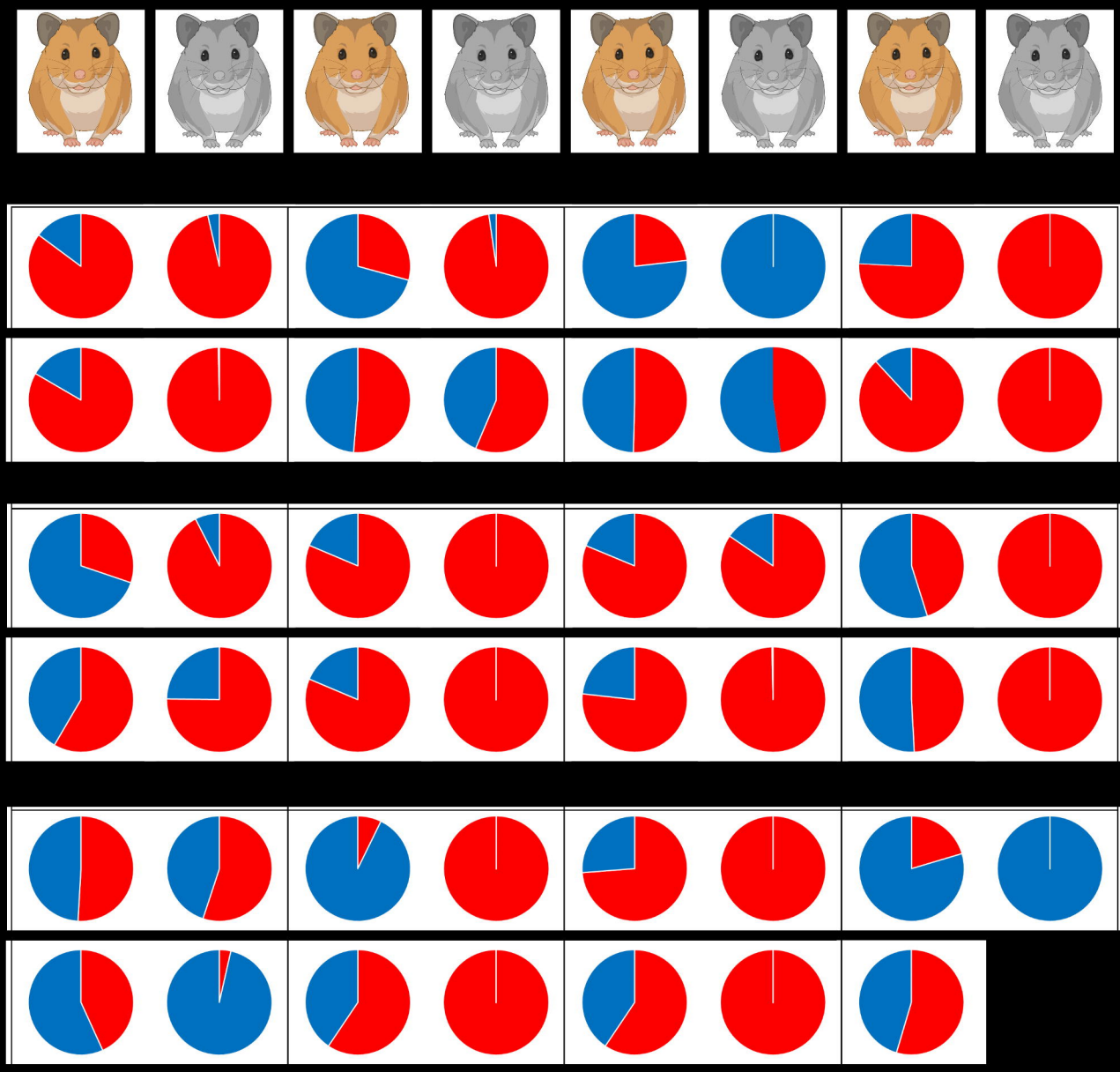
Transmission experiments
BavPat D614G (50%)
+
20I/501Y.V1 (50%)
Infection
40 TCID50
Donors
0
1
2
3
Nasal wash
Lung
Co-housing
6h.
Contacts
0
1
2
3